Steric and Electronic Control of Dynamic Processes in Aryl-Bridged Dicyclooctatetraenes and Their Dianions

Stuart W. Staley,*,† Joanne D. Kehlbeck,† Russell A. Grimm,† Rachel A. Sablosky,† Patrik Boman,‡ and Bertil Eliasson‡

Contribution from the Departments of Chemistry, Carnegie Mellon University, Pittsburgh, Pennsylvania 15213, and Umeå University, S-901 87, Umeå, Sweden

Received March 19, 1998

Abstract: The rate constants for ring inversion ($k_{r.i.}$) and bond shift ($k_{b.s.}$) in **1** and **2** were determined by dynamic NMR spectrometry while the rate constants for bond shift and intramolecular charge transfer ($k_{c.t.}$) were determined for $\mathbf{1}^{2-}/2K^+$ and $\mathbf{2}^{2-}/2K^+$. These processes were modeled by HF/3-21G(*) ab initio molecular orbital calculations of the ground states and of several transition states for **3**, **4**, $\mathbf{3}^{2-}$, $\mathbf{4}^{2-}$, $\mathbf{3}^{2-}/2K^+$, and $\mathbf{4}^{2-}/2K^+$. The results indicate that $k_{r.i.}$ and $k_{b.s.}$ are ca. 2.5 times greater (at 240 and 280 K, respectively) for **2** compared to **1** due to larger steric repulsions in the ground state of **2**. Contrariwise, $k_{b.s.}$ and $k_{c.t.}$ are 1.7 and 166 times greater, respectively, at 280 K for $\mathbf{1}^{2-}/2K^+$ than for $\mathbf{2}^{2-}/2K^+$. These differences are attributed to less twisting and therefore greater π delocalization between the cyclooctatetraenyl rings and the aryl ring in the bond shift and charge-transfer transition states of $\mathbf{1}^{2-}$ compared to $\mathbf{2}^{2-}$. The greater difference between $\mathbf{1}^{2-}$ and $\mathbf{2}^{2-}$ for $k_{c.t.}$ compared to $k_{b.s.}$ is postulated to result from looser ion pairing in the charge-transfer transition state relative to the bond shift transition state.

Bridged dicyclooctratetraene dianions are bistable systems that undergo charge exchange across the bridging organic structural unit.[1] These are excellent systems for assessing the influence of various structural factors on charge transfer and for investigating structural features that could be employed for "tunable" electron transfer.

In addition to charge transfer, bridged dicyclooctatetraenes and their dianions undergo the processes of ring inversion (eq 1) and bond shift (eq 2) common to most cyclooctatetraene

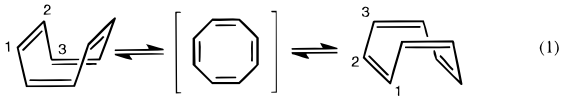

(1)

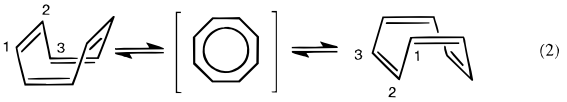

(2)

(COT) rings.[2] In this study, we have compared the energetics of these processes in the 1,4-phenylene- and 1,4-naphthalene-bridged compounds (**1** and **2**, respectively) and their dianions ($\mathbf{1}^{2-}$ and $\mathbf{2}^{2-}$). This comparison has afforded several key insights regarding the relative steric influences of the bridging units in the ground and transition states.

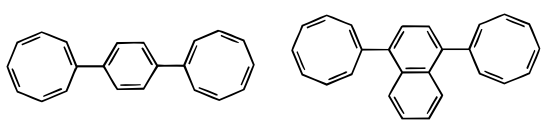

1 **2**

Extensive studies have been made on the effect of bridging groups on the rates of intramolecular energy transfer and electron transfer between donor and acceptor groups. Especially relevant are several studies by Osuka and co-workers on photoinduced zinc-free base hybrid diporphyrins (ZnP−H_2P) and zinc−ferric hybrid diporphyrins (ZnP−Fe^{III}P).[3] These workers determined the rate constants of intramolecular singlet−singlet energy transfer (k_{EN}) from $^1(ZnP)^*$ to H_2P and intramolecular electron transfer (charge separation) (k_{ET}) from $^1(ZnP)^*$ to Fe^{III}P for a series of aryl bridges connecting the porphyrin rings. Of particular interest to the present study are the observations that k_{EN} is 27% larger for the 1,4-phenylene bridge than for the 1,4-naphthalene bridge (6.6 vs 5.2 ($\times 10^{10}$) s^{-1}, respectively)[3a] whereas the relative rate constants are reversed for k_{ET} (ca. 0.8 vs 1.1 ($\times 10^{11}$) s^{-1}).[3b] Calculations of these diporphyrins by Mårtensson that employed various methods of calculating the Förster orientation factor gave identical values of k_{EN} for the two bridges.[4] The origin of these reversed relative rate constants is not known. Another reversal of relative rate constants involving the same two bridging groups is reported for **1** and **2** and their dianions in the present study and an explanation is presented.

Results

Synthesis. 1,4-Dicyclooctatetraenylbenzene (**1**) was prepared by the Pd-catalyzed (Stille) coupling of 1,4-bis(tributylstannyl)-benzene with bromocyclooctatetraene.[5] It was convenient to "reverse" the functional groups for the synthesis of **2** by coupling

† Carnegie Mellon University
‡ Umeå University

(1) (a) Staley, S. W.; Dustman, C. K.; Facchine, K. L.; Linkowski, G. E. *J. Am. Chem. Soc.* **1985**, *107*, 4003. (b) Staley, S. W.; Eliasson, B.; Kearney, P. C.; Schreiman, I. C., Lindsey, J. S. *Molecular Electronic Devices*; Carter, F. L., Siatkowski, R. E., Wohltjen, H., Eds.; Elsevier: Amsterdam, 1988; p 543. (c) Auchter-Krummel, P.; Müllen, K. *Angew. Chem., Int. Ed. Engl.* **1991**, *30*, 1003. (d) Boman, P.; Eliasson, B. *Acta Chem. Scand.* **1996**, *50*, 816.

(2) Review: Paquette, L. A. *Acc. Chem. Res.* **1993**, *26*, 57.

S0002-7863(98)00931-7 CCC: $15.00
Published on Web 09/11/1998

Scheme 1

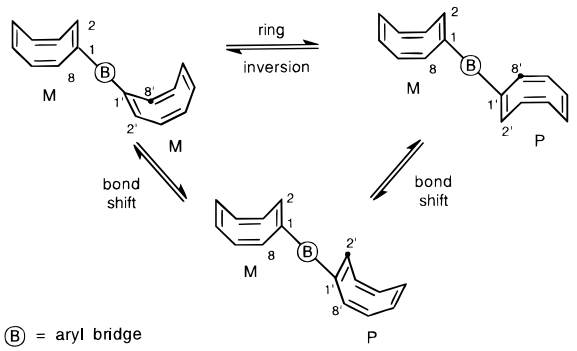

1,4-dibromonaphthalene with trimethylstannylcyclooctatetraene.

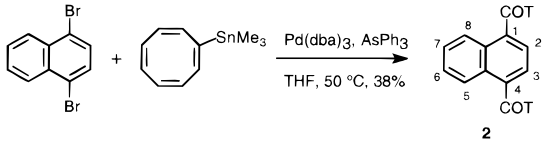

2

This has the advantage of avoiding the use of the thermally labile bromocyclooctatetraene,[6] thereby allowing the reaction to be run at an elevated temperature.

Kinetic Studies. (A) Neutral Dicyclooctatetraenyl Compounds. The COT rings in **1** and **2** adopt a tub-shaped conformation with localized π bonds. Monosubstituted COTs are chiral moieties; consequently diCOT compounds such as **1** and **2** exist as pairs of diastereomers. The enantiomers of a monosubstituted COT can be interconverted either by ring inversion or by π bond shift, both of which occur through a planar transition state (Scheme 1). The stereodescriptors in Scheme 1 (M = minus, P = plus) refer to the helical sense across the substituted chiral axis (the C_1C_8 bond), as defined by the highest priority substituents (C_1═C_2 at C_1 and C_8═C_7 at C_8) according to the Cahn−Ingold−Prelog convention.[7]

Owing to the energy required for ring flattening, both processes occur at rates that affect NMR line widths at accessible temperatures. If the COT rings are in close enough proximity (i.e., if their magnetic environments are sufficiently different), it is possible to detect different ^{1}H or ^{13}C signals for each diastereomer in the slow-exchange region. For example, **1** exhibits eight closely spaced pairs of COT ^{13}C peaks as well as pairs of peaks for the carbons of the aryl bridge at <−50 °C. As the temperature is raised and ring inversion becomes fast on the NMR time scale, the separate signals of the diastereomers coalesce. However, exchange of C_2 with C_8, C_3 with C_7, and C_4 with C_6 due to bond shift is still slow and eight COT carbons are detected in the ^{13}C NMR spectrum from −30 to 20 °C. At still higher temperatures, where bond shift is fast on the NMR time scale, the signals for the above three pairs of carbons are expected to coalesce and only five COT resonances would be observed.

(1) Ring Inversion. Rate constants for the exchange of diastereomers (k_c) were calculated at the two-site coalescence temperatures (T_c) as described in the Experimental Section.

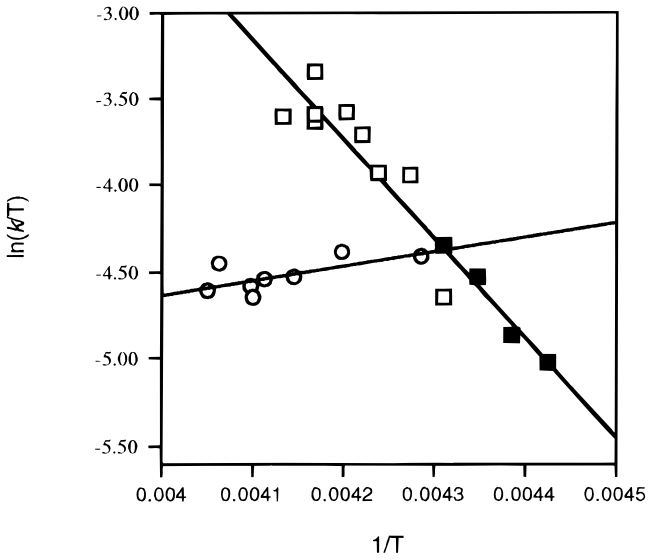

Figure 1. Plots of $\ln(k_c/T)$ vs $1/T$ for the interconversion of diastereomers of **1** and **2**: open circles and squares are for **1** and **2**, respectively, obtained from measurements of T_c, and filled squares are for **2**, obtained by total line shape analysis; $r = 0.671$ (**1**) and 0.960 (**2**).

Since the diastereomers can interconvert through either ring inversion or bond shift, k_c is given by eq 3[8]

$$k_c = k_{r.i.} + k_{b.s.}/2 \qquad (3)$$

(see Scheme 1). Values for $k_{b.s.}$ (vide infra) were determined for at least four temperatures over a 25 degree range and extrapolated to T_c to calculate $k_{r.i.}$.

At temperatures where ring inversion is slow on the ^{13}C NMR time scale (<−50 °C), each diastereomer of **1** exhibits ten signals (8 COT and 2 aryl) in the ^{13}C NMR spectrum, four of which (δ 132.9, 132.5, 128.7, and 126.7) were sufficiently separated to permit investigation of coalescence over a 13.5 degree temperature range. Similar behavior was observed by ^{1}H NMR spectrometry. Severe signal overlap in the COT region (δ 5.8−6.2) prohibited extraction of kinetic data from these signals. However, the singlet at δ 7.31 due to the protons on the phenylene bridge splits into a pair of singlets below −60 °C.

Analogous behavior can be observed for **2**. At temperatures where ring inversion is slow on the NMR time scale (<−60 °C), the two diastereomers are expected to exhibit 13 pairs of ^{13}C signals (8 COT and 5 aryl). At 75 MHz, however, only nine pairs are free from overlap while the remaining signals are superimposed at δ 132.8. Four signals (δ 144.2, 133.9, 132.0, and 126.2) were sufficiently separated to permit investigation of coalescence.

In the ^{1}H NMR spectrum, the downfield half of the AA′BB′ multiplet, which we assign to H_5 and H_8 of the naphthalene bridge, exhibits broadening at low temperatures, but T_c was not reached down to −90 °C. The upfield half of the AA′BB′ multiplet remained coalesced down to −80 °C. However, the singlet at δ 7.23 due to the naphthyl protons ortho to the COT rings (H_2 and H_3) splits into a pair of singlets below −40 °C. Total line shape analysis of these signals over a 15 degree temperature range provided several values for $k_{r.i.}$.

(2) Bond Shift. Bond shift rate constants were calculated at a number of temperatures where line broadening could be measured in the slow exchange regime. The rate constants for

(3) (a) Osuka, A.; Maruyama, K.; Yamazaki, I.; Tamai, N. *Chem. Phys. Lett.* **1990**, *165*, 392. (b) Osuka, A.; Maruyama, K.; Mataga, N.; Asahi, T.; Yamazaki, I.; Tamai, N. *J. Am. Chem. Soc.* **1990**, *112*, 4958.

(4) Mårtensson, J. *Chem. Phys. Lett.* **1994**, *229*, 449.

(5) Siesel, D. A.; Staley, S. W. *J. Org. Chem.* **1993**, *58*, 7870.

(6) Gasteiger, J.; Gream, G. E.; Huisgen, R.; Konz, W. E.; Schnegg, U. *Chem. Ber.* **1971**, *104*, 2412.

(7) Cahn, R. S.; Ingold, C.; Prelog, V. *Angew. Chem., Int. Ed. Engl.* **1966**, *5*, 385.

(8) Oth, J. F. M. *Pure Appl. Chem.* **1971**, *25*, 573.

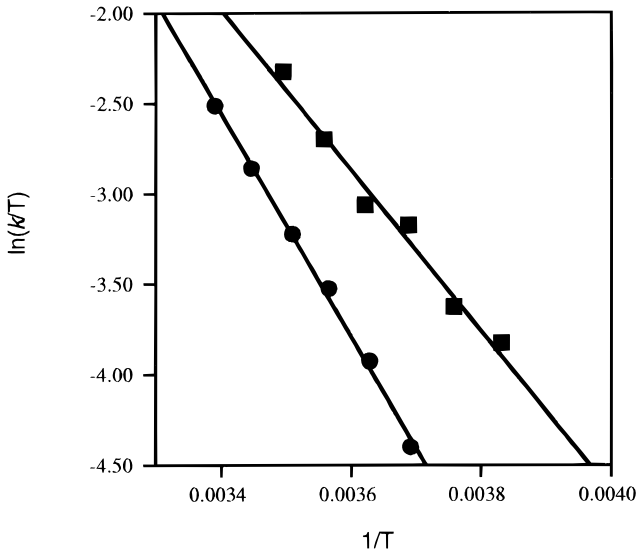

Figure 2. Plots of $\ln(k_{b.s.}/T)$ vs $1/T$ for bond shift in **1** (circles) and **2** (squares); $r = 0.999$ and 0.991, respectively.

Table 1. Kinetic Data for Ring Inversion and Bond Shift in **1** and **2** in THF-d_8

compd	process	T range (K)	k^a	T (K)	$\Delta G^{\ddagger\,b}$
1	r.i.	233−244	2.7	240	13.5 (±0.2)
	b.s.	271−298	7.5	280	15.2 (±0.1)
2	r.i.	226−242	6.7	240	13.0 (±0.2)
	b.s.	261−286	18.2	280	14.7 (±0.1)

[a] In s^{-1}. [b] In kcal/mol.

bond shift in **1** and **2** were determined for four and two samples, respectively. ^{13}C line broadening was measured for six non-overlapping signals (δ 133.6, 133.3, 133.1, 132.5, 132.3, 128.7) in **1** and for three signals (δ 135.8, 132.6, 132.0) in **2**. Values for $k_{b.s.}$ were determined over 27 and 25 degree temperature ranges for **1** and **2**, respectively, as described in the Experimental Section. Although the COT ^{13}C signals had coalesced by 50 °C, five distinct signals were not observed due to overlap.

(B) Dicyclooctatetraenyl Dianions. Dianions $\mathbf{1}^{2-}$ and $\mathbf{2}^{2-}$ were generated by reduction of **1** and **2**, respectively, with potassium metal in sealed NMR tubes. At low temperatures (−40−25 °C) ^{13}C NMR spectra of $\mathbf{1}^{2-}$ and $\mathbf{2}^{2-}$ display eight COT signals for the neutral ring and four or 10 bridge signals, respectively, in the range δ 158−122 as well as five COT dianion ring signals at higher field (δ 102−89).[9] Line broadening due to bond shift was measured over 27 degree temperature ranges for both $\mathbf{1}^{2-}$ and $\mathbf{2}^{2-}$. In the fast exchange regime for bond shift the spectrum would contain five neutral COT signals and five COT dianion signals as well as bridge signals, although the signals for the neutral ring had not emerged from the baseline by 50 °C. Intramolecular inter-ring exchange due to charge transfer occurs upon further warming (>50 °C) and affects all COT signals as well as those for the bridge. Charge transfer is *intramolecular*, as evidenced by the observation that $k_{c.t.}$ does not change over a 5-fold increase in the concentration of $\mathbf{2}^{2-}$.

(1) Bond Shift. The rate constants for bond shift in $\mathbf{1}^{2-}$ and $\mathbf{2}^{2-}$ were determined for two and four samples, respectively, and are listed in Table 2. ^{13}C line broadening was measured for six signals (δ 134.9, 134.0, 132.5, 132.2, 131.0, 122.2) over a 27 degree temperature range for $\mathbf{1}^{2-}$ and for 4−6 signals (δ 137.2, 133.5, 133.1, 132.0, 131.3, 130.8) over a 26.5 degree temperature range for $\mathbf{2}^{2-}$.

(9) One or more dynamic processes affect the ^{13}C signals of the dianion ring of $\mathbf{2}^{2-}$ below −40 °C. This will be discussed in detail in a future publication.

Table 2. Kinetic Data for Bond Shift and Charge Transfer in $\mathbf{1}^{2-}/2K^+$ and $\mathbf{2}^{2-}/2K^+$ in THF-d_8

compd	process	T range (K)	k^a	T (K)	$\Delta G^{\ddagger\,b}$
$\mathbf{1}^{2-}/2K^+$	b.s.	248−284	43.3	280	14.3 (±0.1)
	c.t.		0.055	280	18.0[c]
	c.t.	313−331	3.4	335	18.9 (±0.2)
$\mathbf{2}^{2-}/2K^+$	b.s.	251−283	25.7	280	14.6 (±0.1)
	c.t.		0.00033	280	20.8[c]
	c.t.	329−344	0.11	335	21.2 (±0.2)

[a] In s^{-1}. [b] In kcal/mol. [c] Extrapolated.

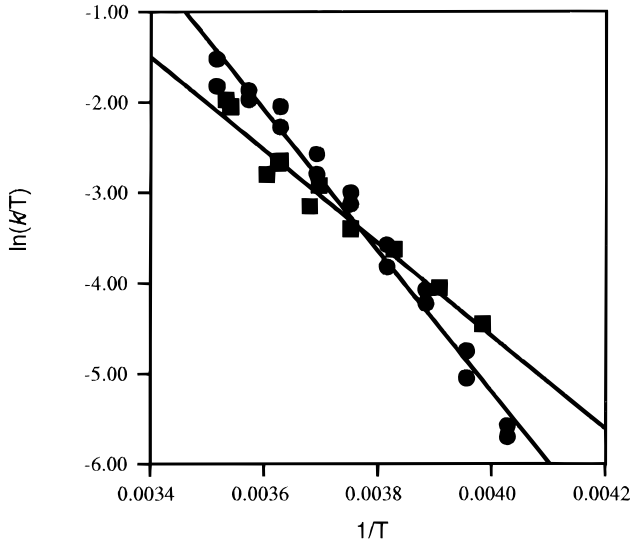

Figure 3. Plots of $\ln(k_{b.s.}/T)$ vs $1/T$ for bond shift in $\mathbf{1}^{2-}$ (circles) and $\mathbf{2}^{2-}$ (squares); $r = 0.989$ and 0.982, respectively.

(2) Charge Transfer. Magnetization transfer methods are particularly appropriate for the measurement of $k_{c.t.}$ in this study because of their insensitivity to the presence of adventitious radicals.[10] The rate constants for charge transfer in $\mathbf{2}^{2-}$ were measured by ^1H spin saturation transfer (SST) over a temperature range of 15 degrees on four samples that ranged in concentration from 0.08 to 0.5 M. The doublets for the exchanging naphthyl protons peri to the COT rings at δ 8.60 and 8.18 (H_5 and H_8) were investigated. One signal was saturated while the change in intensity of its exchange partner was monitored and the roles of the two protons were interchanged on alternate experiments. (See Experimental Section for details.) The other pairs of exchanging bridge protons exhibited NOE effects and could not be used to extract kinetic information by ^1H SST. Severe signal overlap in the region of the COT proton signals (δ 5.8−6.2) prevented extraction of kinetic data by SST from these signals.

Detectable NOE effects also prevented the use of ^1H SST on the exchanging aryl signals of $\mathbf{1}^{2-}$. Therefore, $k_{c.t.}$ was measured by ^{13}C inversion transfer (IT), as described in the Experimental Section. The signal for C_5 was inverted and the peak heights of C_5 and $C_{5'}$ were monitored as a function of delay time. Rate constants were measured over a temperature range of 18 degrees on two separate samples.

(C) Treatment of Kinetic Data. The rate constants obtained at various temperatures from the above studies are given in the Supporting Information. Plots of $\ln(k/T)$ vs $1/T$ gave good correlations and are presented in Figures 1−4. Rate constants for the neutral molecules and for the dianions at common temperatures were calculated from the regression lines in Figures

(10) Boman, P.; Eliasson, B.; Grimm, R. A.; Staley, S. W. Unpublished results.

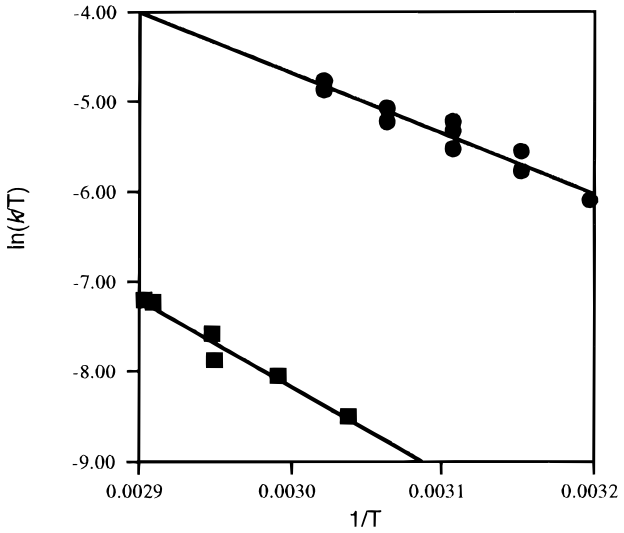

Figure 4. Plots of $\ln(k_{c.t.}/T)$ vs $1/T$ for bond shift in $\mathbf{1}^{2-}$ (circles) and $\mathbf{2}^{2-}$ (squares); $r = 0.962$ and 0.976, respectively.

1−4 and are given in Tables 1 and 2, respectively. Care was taken to minimize extrapolations beyond the experimental temperature ranges. Free energies of activation ($\Delta G^{\ddagger}$) were calculated from the rate constants by using the Eyring equation (eq 4).[11]

$$\Delta G^{\ddagger} = (4.575 \times 10^{-3})T[10.319 + \log(T/k)] \qquad (4)$$

Discussion

The kinetic data (Table 1) show that **2** undergoes ring inversion and bond shift ca. 2.5 times faster than **1** at 280 K. Contrariwise, bond shift is 1.7 times faster in $\mathbf{1}^{2-}$ than in $\mathbf{2}^{2-}$, while the former dianion undergoes charge transfer over 166 times faster than $\mathbf{2}^{2-}$ (Table 2). Thus there is a relative change in rate constants between **1** and **2** of *ca. 400* on comparing ring inversion or bond shift in the neutral molecules with charge transfer in the dianions.

To assess the steric factors involved in these processes, we performed HF/3-21G(*) [12] geometry optimizations and harmonic frequency analyses[13] on the ground-state conformations and ring inversion transition states[14] of phenylCOT (**3**) and 1-naphthyl-COT (**4**) and on the ground state conformations for uncomplexed and dipotassium-complexed $\mathbf{3}^{2-}$ and $\mathbf{4}^{2-}$. These compounds are good model compounds for **1**, **2**, $\mathbf{1}^{2-}$, and $\mathbf{2}^{2-}$, respectively. Optimization of the latter compounds would be very complex owing to their large size and to the existence of multiple conformational minima and (for **1** and **2**) two diastereomers.

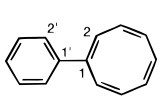

3

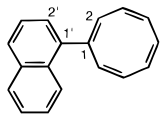

4

As shown in Tables S1 and S2 of the Supporting Information, optimized structures of $\mathbf{3}^{2-}/2K^{+}$ and the ground and ring inversion transition states of **3** have almost the same degree of twist (within 0.3° at the semiempirical AM1 level and 1.3° at the ab initio HF/3-21G(*) level) as in the corresponding structures for $\mathbf{1}^{2-}/2K^{+}$ and **1.** However, the HF/3-21G(*) optimizations afforded minimum energy structures that are 4−9° more twisted than the corresponding AM1-optimized structures. We therefore deemed it preferable to calculate the model compounds at HF/3-21G(*) than to calculate **1** and **2** and their dianions at the lower AM1 level.

The calculated relative energies of the ground states and ring inversion transition states, corrected for zero point energies ($\Delta E_{r.i.} + \Delta ZPE$), as well as the optimized twist angles between the COT or COT dianion ring and the phenyl or naphthyl ring, are given in Table 3. Note that $\Delta(\Delta E_{r.i.} + \Delta ZPE)$ calculated for **3** relative to **4** (1.1 kcal/mol) is similar to the corresponding difference measured for $\Delta G^{\ddagger}_{r.i.}$ in **1** and **2** (0.5 kcal/mol), indicating that the calculations reliably reproduce the *relative* ground and transition state energies and structures.

As seen in Table 3, the twist angle in **3** increases by nearly 20° on going from the ground state to the ring inversion transition state. This results from increased interactions between H_2 and H_8 of the COT ring and the ortho hydrogens of the phenyl ring that are caused by (a) an increase of $\angle C_2C_1C_8$ from 126° in the tub-like ground state to 135° in the planar transition state and (b) a decrease in the dihedral angle between the C_8-H_8 bond and the C_1−phenyl bond from 50° in the ground state to 0° in the ring inversion transition state.

In contrast, the degree of twist of the naphthyl group, which primarily results from interactions of H_8 of the naphthyl group with the COT ring, remains essentially unchanged at 76−77° on going to the transition state. The minimum energy conformations of **4** are illustrated in Figure 5. Since, in the absence of strong conjugation, the twist angle largely reflects the amount of steric hindrance between adjacent rings, the calculated twist angles indicate that inter-ring steric effects increase on going to the ring inversion transition state in **1** but are unchanged in **2**. Presumably the same conclusion applies to the structurally similar bond shift transition states, which we were not able to calculate because large multiconfiguration wave functions are required.[15] The relative rates of ring inversion and bond shift in **1** and **2** can be said to be *primarily controlled by differences in ground-state steric effects*.

The COT dianion is a stronger donor than the neutral COT ring. Furthermore, the donor ability of the dianion undoubtedly varies as a function of its ion pairing. For example, a COT dianion complexed with two potassium cations is calculated to have twist angles of 46° and 58° with phenyl and 1-naphthyl, respectively, whereas these angles decrease to 29° and 35°, respectively, in the uncomplexed dianions (Table 3). The former calculation serves as a model for a contact ion-paired dianion whereas the latter models a solvent-separated ion pair.

Compound $\mathbf{1}^{2-}$ is slightly more susceptible than $\mathbf{2}^{2-}$ to bond shift in the neutral ring and substantially more susceptible to intramolecular charge transfer. Since approximately the same steric interactions are present between the neutral COT rings

(11) Sandstrom, J. *Dynamic NMR Spectroscopy*; Academic: New York, 1982; pp 14−18, 96.

(12) (a) Binkley, J. S.; Pople, J. A.; Hehre, W. J. *J. Am. Chem. Soc*. **1980**, *102*, 939. (b) Pietro, W. J.; Francl, M. M.; Hehre, W. J.; DeFrees, D. J.; Pople, J. A.; Binkley, J. S. *J. Am. Chem. Soc.* **1982**, *104*, 5039. (c) Gordon, M. S.; Binkley, J. S.; Pople, J. A.; Pietro, W. J.; Hehre, W. J. *J. Am. Chem. Soc*. **1982**, *104*, 2797. (d) Dobbs, K. D.; Hehre, W. J. *J. Comput. Chem*. **1986**, *7*, 359.

(13) Frisch, M. J.; Trucks, G. W.; Schlegel, H. B.; Gill, P. M. W.; Johnson, B. G.; Wong, M. W.; Foresman, J. B.; Robb, M. A.; Head-Gordon, M.; Replogle, E. S.; Gomperts, R.; Andreas, J. L.; Raghavachari, K.; Binkley, J. S.; Gonzalez, C.; Martin, R. L.; Fox, D. J.; Defrees, D. J.; Baker, J.; Stewart, J. J. P.; Pople, J. A. *Gaussian 92/DFT, Revision G.1*; Gaussian, Inc.: Pittsburgh, PA, 1993.

(14) Since Karadakov et al. found that the CASSCF/6-31G*//HF/6-31G correlation energy for the D_{4h} ring inversion transition state of COT is only 3% greater than that for the D_{2d} ground state, we conclude that relative values of $\Delta E_{r.i.}$ can be reliably calculated at the HF level of theory; Karadakov, P. B.; Gerratt, J.; Cooper, D. L.; Raimondi, M. *J. Phys. Chem*. **1995**, *99*, 10186.

(15) Hrovat, D. A.; Borden, W. T. *J. Am. Chem. Soc*. **1992**, *114*, 5879.

Table 3. Relative Energies and Torsional Angles for the Optimized HF/3-21G Ground States and Ring Inversion Transition States (T.S.) of **3** and **4** and Their Dianions

compd[a]	$\Delta E_{r.i.} + \Delta ZPE$[b]	$C_1-C_{1'}-C_{2'}$-aryl torsional angle[c]
3	0	44.4
T. S.	18.9	63.7
4	0	−77.1[d]
	0.4	89.3[e]
T. S.	17.8	75.9
$\mathbf{3}^{2-}$		28.6
$\mathbf{4}^{2-}$		35.2
$\mathbf{3}^{2-}/2K^{+}$[f]		46.2
$\mathbf{4}^{2-}/2K^{+}$[f]		57.7

[a] Ground state (no imaginary frequencies) unless indicated otherwise. [b] In kcal/mol relative to the ground state. [c] $\omega(C_2C_1C_{1'}C_{2'})$, in degrees. [d] Conformation 1; $C_{2'}$ is rotated as in Figure 5 (left). [e] Conformation 2; $C_{2'}$ is rotated as in Figure 5 (right). [f] The potassium ions were fixed in the positions found for $COT^{2-}/2K^{+}$ by X-ray diffraction[28] and all other parameters were optimized. An HF/3-21G(*) basis set[12d] was employed for potassium.

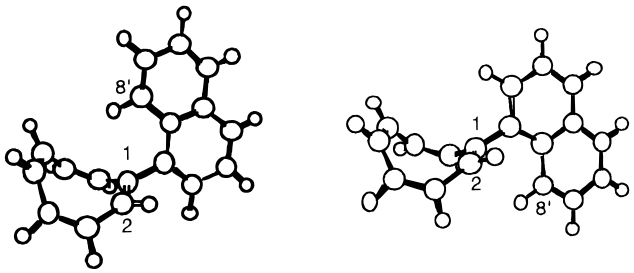

Figure 5. HF/3-21G geometry-optimized conformations for **4**. Left: Global minimum; the naphthyl group is rotated upward by 77.1° from the conformation where $C_{8'}$ is farthest from C_2 of the COT ring. Right: The naphthyl group is rotated downward by 89.3° from the conformation where $C_{8'}$ is farthest from C_2.

and the aryl bridge of the ground states of $\mathbf{1}^{2-}$ and $\mathbf{2}^{2-}$ as in those of **1** and **2**, respectively, *the relative bond shift and charge-transfer rate constants of the dianions must be controlled by steric and electronic effects in the transition states*. The acceptor character of the neutral COT ring increases substantially in the bond shift transition state owing to the interaction of a low-lying unoccupied π molecular orbital with the electron-rich substituent. This causes a greater driving force for π-electron delocalization and, consequently, a smaller twist angle than in the ground state. Note that the degree of twist in transition state models $\mathbf{3}^{2-}$ and $\mathbf{4}^{2-}$ is probably overestimated since the models employed the structures of the ring inversion rather than the bond shift transition states.

The greater difference in $k_{c.t.}$ for $\mathbf{1}^{2-}$ and $\mathbf{2}^{2-}$ relative to $k_{b.s.}$ can be understood as follows. The charge transfer process must involve transfer of the counterions, which are probably more solvated in the transition state (even though they may still be contact ion pairs[16]) than in the ground state. On the other hand, bond shift in the dianion does not require cation migration and its transition state is therefore more tightly ion paired than that for charge transfer. A looser COT dianion ion pair is a stronger donor group than a cation-complexed dianion, as indicated by the smaller twist angles calculated for the uncomplexed dianions (Table 3). Therefore, we conclude that *the greater difference in $k_{c.t.}$ for $\mathbf{1}^{2-}$ and $\mathbf{2}^{2-}$ compared to $k_{b.s.}$ is due to looser ion pairing in the charge-transfer transition state relative to the bond shift transition state.*

(16) Staley, S. W.; Grimm, R. A.; Boman, P.; Eliasson, B. Manuscript in preparation.

Experimental Section

General. THF was distilled from sodium metal/benzophenone ketyl. Preparative flash column chromatography was performed on 40 μM silica gel (SG). NMR spectra were obtained at 300 or 360 MHz for ^{1}H and 75 or 90 MHz for ^{13}C on a GE GN 300 NMR spectrometer in Pittsburgh or a Bruker 360 NMR in Umeå, respectively. Elemental analyses were performed by Midwest Microlabs, Inc., Indianapolis, IN.

1,4-Dicyclooctatetraenylbenzene (1) was prepared according to the published procedure.[5]

1,4-Dicyclooctatetraenylnaphthalene (2). To a solution of 1,4-dibromonaphthalene (0.715 g, 2.50 mmol), Pd_2dba_3 (0.114 g, 0.125 mmol), and $AsPh_3$ (0.306 g, 1.00 mmol) in 25 mL of anhydrous THF at 50 °C was added cyclooctatetraenyltrimethylstannane[17] (1.339 g, 5.00 mmol) in 5 mL of dry THF. After 24 h the reaction mixture was diluted with 50 mL of Et_2O and 50 mL of 50% saturated aqueous KF was added. The mixture was stirred for 15 min and filtered and the organic layer was washed with 1 × 50 mL of 50% saturated aqueous KF, 2 × 50 mL of H_2O, and 1 × 50 mL of brine. The combined aqueous layers were extracted with 25 mL of Et_2O and the combined organic layers were dried ($MgSO_4$) and concentrated. The residue was dissolved in 200 mL of CH_2Cl_2/hexane and 4 g of SG was added. The solvent was then removed by rotary evaporation and the residue was chromatographed on 50 g of SG with 5% CH_2Cl_2/hexane to afford 300 mg (36%) of a light yellow solid: mp 124−124.5 °C; IR 3064, 3039, 3001, 1630, 1508, 1371, 808, 764, 680, 620 cm^{-1}; UV λ_{max}(cyclohexane) 300 nm (ϵ 13 600); ^{1}H NMR (THF-d_8, 25 °C) δ 5.8−6.1 (m, 14H), 7.22 (s, 2H), 7.45 and 8.34 (AA′BB′, 4H). Simulation of a spectrum obtained at −30 °C gave the following:[18] $J_{AA'} = 0.2$ Hz, $J_{AB'} = 0.7$ Hz, $J_{AB} = 6.5$ Hz, $J_{BB'} = 6.7$ Hz; ^{13}C NMR (THF-d_8, −30 °C) δ 144.16, 140.95, *135.81*, 133.87, *132.85*, *132.80* (2 signals overlapped), *132.62*, 132.23, *131.97*, 127.12, 126.36, 126.14. The italicized values are those for C_2-C_4 and C_6-C_8, which undergo exchange during bond shift. TLC (5% CH_2Cl_2/hexane): $R_f = 0.2$. Anal. Calcd for $C_{26}H_{20}$: C, 93.94; H, 6.06. Found: C, 93.74; H, 6.09.

Preparation of NMR Samples. Samples of $\mathbf{1}^{2-}/2K^{+}$ and $\mathbf{2}^{2-}/2K^{+}$ were prepared directly in lengthened 5 mm NMR tubes by reduction of **1** and **2**, respectively, with potassium metal. A small glass wool plug was inserted into the upper part of an NMR tube containing **1** or **2**, THF-d_8, and approximately 5 μL of cyclohexane. An excess of alkali metal was placed on top of the glass wool and the sample was degassed with 5 freeze−pump−thaw cycles and sealed under an atmosphere of argon. A mirror of metal was then formed by freezing the solution in liquid nitrogen and heating the tube above the metal with a gentle flame. Agitation of the tube to bring the metal into contact with the heated glass produced a mirror. After cooling, reduction was initiated by inverting the tube to allow the solution to filter through the glass wool plug and come into contact with the potassium mirror. The tube was inverted repeatedly until the proper reduction stage was reached as judged from the ^{1}H NMR spectrum. NMR spectra of dianion samples stored in a freezer typically showed no decomposition over periods of several months.

Dipotassium Salt of 1,4-Dicyclooctatetraenylbenzene ($\mathbf{1}^{2-}/2K^{+}$). ^{1}H NMR (THF-d_8, 0 °C) δ 5.5−6.6 (m, 7H, H_{2-8}), 5.42 (t, $J = 10.5$ Hz, 1H, $H_{5'}$), 5.62 (t, $J = 10.6$ Hz, 2H) and 5.72 (t, $J = 10.6$ Hz, 2H) ($H_{3'}$, $H_{4'}$, $H_{6'}$, $H_{7'}$), 6.00 (t, $J = 11.5$ Hz, 2H, $H_{2'}$ and $H_{8'}$), 6.85 (d, $J = 8.7$ Hz, 2H) and 7.34 (d, $J = 8.7$ Hz, 2H) (aryl Hs, H_{10} and H_{11}). ^{13}C NMR (THF-d_8, −60 °C) δ 91.20 ($C_{2'}$), 91.23 and 94.51 ($C_{3'}$, $C_{4'}$), 95.65 ($C_{5'}$), 102.22 ($C_{1'}$), *122.20*, 124.86 and 127.64 (C_{10}, C_{11}), 128.99 and 157.06 (C_9, C_{12}), *130.97*, *132.15*, 132.78 (C_5), *132.51*, *134.02*, *134.91*, 142.97 (C_1). The italicized values are those for C_2-C_4 and C_6-C_8, which undergo exchange during bond shift.

Dipotassium Salt of 1,4-Dicyclooctatetraenylnaphthalene ($\mathbf{2}^{2-}/2K^{+}$). ^{1}H NMR (THF-d_8, 0 °C) δ 5.5−6.2 (m, 14H) (H_{2-8}, $H_{2'-8'}$), 7.03 (d, $J = 5.4$ Hz, 1H), 7.08 (t, $J = 5.9$ Hz, 1H), 7.17 (t, $J = 5.9$ Hz, 1H), 7.40 (d, $J = 5.4$ Hz, 1H), 8.16 (d, $J = 5.9$ Hz, 1H) and 8.60 (d, $J = 5.9$ Hz, 1H) (peri Hs, H_5 and H_8). ^{13}C NMR (THF-d_8, −40 °C) δ

(17) Cooke, M.; Russ, C. R.; Stone, F. G. A. *J. Chem. Soc., Dalton Trans.* **1975**, 256.

(18) Budzelaar, P. H. M. *gNMR Version 3.6 for Macintosh*; Cherwell Scientific Publishing Limited, copyright gNMR, Ivory Soft, 1996.

158.38, 146.14, *137.15*, 134.05, 133.66 (C_5), *133.51*, *133.09*, 132.88, *132.04*, 131.95, 131.89, *131.28*, *130.79*, 128.88, 126.06, 124.95, 124.04, 122.88, 102.18 ($C_{1'}$), 95.45, 93.52 ($C_{5'}$), 92.09, 89.85. The italicized values are those for C_2-C_4 and C_6-C_8, which undergo exchange during bond shift.

Kinetic Methods. General. All kinetics were measured for at least two independent samples. The temperature was determined from the difference in the proton chemical shifts of methanol for temperatures <295 K or from the corresponding difference for ethylene glycol for temperatures >295 K according to the method of van Geet.[19] The temperature accuracy is estimated to be ±1 °C due to improvements made to the variable-temperature system as recommended by Allerhand.[20] The free induction signals were sampled with 32K data points. After zero filling and Fourier transformation, the spectral resolution was typically in the range of 0.3−0.5 Hz/point.

Line Broadening. Bond shift rate constants ($k_{b.s.}$) were calculated at a number of temperatures from ^{13}C signals where line broadening could be determined. Line widths for the pairwise exchanging carbons (C_2 and C_8, C_3 and C_7, C_4 and C_6) could each, in principle, be measured, but $k_{b.s.}$ was determined only for signals with no overlap. Rate constants for bond shift were calculated by eq 5,[11]

$$k_{b.s.} = \pi \Delta W_{ex} \tag{5}$$

where ΔW_{ex} is the exchange broadening of a signal (in Hz) in the region of slow exchange. ΔW_{ex} is the observed line width at half-height ($W_{1/2}$) corrected for the intrinsic line width. This correction was accomplished in one of two ways. From spectra at low temperature, where bond shift exchange broadening was absent, it was found that the line width of C_5 was very similar to those of the other proton-bearing carbons in the neutral ring. At higher temperatures, the line width of C_5, which does not undergo exchange, was subtracted from the line width of the exchange-broadened signals to give ΔW_{ex}. Alternatively, an internal reference can be used to correct for the intrinsic line width when C_5 is overlapped by other signals. The exchange broadening was determined by eq 6,

$$\Delta W_{ex} = W_{1/2} - W_0 - (W_{ref'} - W_{ref}) \tag{6}$$

where W_o is the line width of an exchanging signal at a temperature below where exchange broadening is observed and the term ($W_{ref'} - W_{ref}$) corrects for solvent viscosity and instrumental inhomogeneity effects. $W_{ref'}$ is the line width of the reference signal at each temperature at which broadening is measured, and W_{ref} is the line width of the reference signal at a temperature below where exchange broadening is observed. The reference line width used in this study was that for cyclohexane. Although cyclohexane has the advantages that it is well upfield from the cyclooctatetraene signals and gives a sharp signal at low concentration, the use of C_5 in determining ΔW_{ex} is preferred owing to its similarity to the exchanging carbons, and was used whenever it was free from overlapping signals. Cases where both methods of correction could be employed yielded identical values for ΔW_{ex}. All line widths were determined by a least-squares fit of the peak to a Lorentzian line shape.

Coalescence Measurements. The rate of interconversion of two singlets at the coalescence temperature (k_c) was obtained from eq 7,[21]

$$k_c = \pi \delta \nu / \sqrt{2} \tag{7}$$

where $\delta\nu$ is the difference (in Hz) between the chemical shifts of the exchanging signals. Values of $\delta\nu$ were measured at a number of temperatures below coalescence and the value at coalescence was then determined by extrapolation of the regression line.

Total Line Shape Analysis. Total line shape analysis of the ^1H NMR spectra was performed on nonoverlapping signals. The line shapes resulting from the broadening of ^1H signals near coalescence were visually compared with calculated spectra obtained with the computer program gNMR.[18] Chemical shifts, coupling constants, and intrinsic relaxation times of the nuclei undergoing exchange were estimated from experimental spectra. The rate constant for exchange (k_{ex}) was then systematically varied to achieve the best visual fit of the calculated with the experimental spectra.

Magnetization Transfer. Two magnetization transfer experiments, spin saturation transfer (SST) and inversion transfer (IT), were employed to determine $k_{c.t.}$. For the ^1H SST experiment, the intensity (I) of one signal of an exchanging pair (nucleus i) was measured while selectively saturating its exchange partner (nucleus s) with low-power homodecoupling. The equilibrium, or off-resonance, intensities ($I°$) of i were obtained while irradiating at a frequency $|\delta_i - \delta_s|$ from site i (i.e., at an equal frequency difference on the other side of nucleus i) to correct for decoupler spillover due to the decoupler's frequency bandwidth. While saturating site s, apparent spin−lattice relaxation times (T_{1app}) of site i were measured by the inversion recovery method (180°−τ−90°).

The intensity reduction determined for exchange by charge transfer must be absent of interfering nuclear Overhauser enhancements. Therefore, NOE effects were qualitatively measured at temperatures below where charge transfer could be detected and care was taken not to use pairs of exchanging signals with detectable NOE effects. The same baseline and scaling factors were used in all spectra to ensure that intensities were reproducible. Intensities were based on peak heights rather than integrated areas since the former are more accurate.[22]

Rate constants for charge transfer were calculated according to eq 8

$$k_{c.t.} = (I° - I)/I°(1/T_{1app}) \tag{8}$$

where $(I° - I)/I°$ is the fractional decrease in intensity of resonance i upon saturation of resonance s and $1/T_{1app}$ is the reciprocal of the apparent spin−lattice relaxation time of i while saturating s. At least 10 measurements at each temperature were averaged to obtain a fractional decrease in peak height. Three measurements of T_{1app} were averaged to arrive at the reported values.

For the ^{13}C IT experiment, $k_{c.t.}$ was obtained by simultaneously fitting Campbell's solution to the McConnell-modified Bloch equations as given in eqs 9−11.[23]

$$I_Z = Ae^{\lambda_+ t} + Ae^{\lambda_- t} + I_\infty \tag{9}$$

$$S_Z = \frac{A(\rho_I + k + \lambda_+)e^{\lambda_+ t}}{k} + \frac{A(\rho_S + k + \lambda_+)e^{\lambda_- t}}{k} + S_\infty \tag{10}$$

$$\lambda_\pm = -{}^1/_2(\rho_I + \rho_S + 2k) \pm \{[\rho_I - \rho_S]^2 + 4k^2\}^{1/2} \tag{11}$$

Here I_Z and S_Z are the instantaneous values of the z magnetization of nuclei I and S as given by the peak heights, I_∞ and S_∞ are the equilibrium ($t = \infty$) values of the z magnetization of I and S, ρ_I and ρ_S are the relaxation rate constants for I and S, and the constants A and B are given by the initial ($t = 0$) z magnetization of I and S. The peak heights of the exchanging signals were fit simultaneously and all seven parameters were optimized to yield the rate constant.

Selective inversion of S was achieved by a 90°x−τ−90°x pulse sequence.[24] The carrier frequency was set to the frequency of the peak to be inverted (S) while the delay time (τ) was set equal to $(2|\delta_i - \delta_s|)^{-1}$. The delay between acquisitions was at least five times T_1 of the carbons undergoing exchange to allow for complete relaxation of the system.

The value of T_1 was determined by the inversion recovery method (180°−t−90°).[25] A nonselective 180° pulse was achieved with a 90°x−

(19) (a) Van Geet, A. L. *Anal. Chem.* **1970**, *42*, 679. (b) Van Geet, A. L. *Anal. Chem.* **1968**, *40*, 2227.
(20) Allerhand, A.; Addleman, R. E.; Osman, D. *J. Am. Chem. Soc.* **1985**, *107*, 5809.
(21) Gutowsky, H. S.; Holm, C. H. *J. Chem. Phys*. **1956**, *25*, 1228.
(22) Perrin, C. L.; Thoburn, J. D.; Kresge, A. J. *J. Am. Chem. Soc*. **1992**, *114*, 8800.
(23) (a) Led, J. J.; Neesgaard, E.; Johansen, J. T. *FEBS Lett.* **1982**, *147*, 74. (b) Campbell, I. D.; Dobson, C. M.; Ratcliffe, R. G.; Williams, R. J. P. *J. Magn. Reson.* **1978**, *29*, 397.
(24) Robinson, G.; Kuchel, P. W.; Chapman, B. E.; Doddrell, D. M.; Irving, M. G. *J. Magn. Reson.* **1985**, *29*, 397.
(25) Levy, G. C.; Peat, I. R., *J. Magn. Reson.* **1975**, *18*, 500.

180°y−90°x composite pulse sequence.[26] The signal intensities were fit to a three-parameter variation of the standard recovery equation (eq 12),

$$M_z^t = M_o\{1 - [1 - k(1 - e^{-AT/T_1})]e^{-t/T_1}\} \quad (12)$$

where M_o is the magnetization when $t \gg T_1$, k is a measure of the imperfections of the rf pulse ($k = -$(amplitude at $t = 0$)/M_o), and AT is the data acquisition time.[25] This method has the advantage over the standard two-parameter variation method of correcting for incomplete 180° inversion.

The uncertainties in the rate constants were estimated from replicate measurements because differential error analysis yielded unreasonably small uncertainties in the rate constants. The error in $\Delta G^{\ddagger}$ was determined by propagation of the errors from the rate constants. The maximum error in k has been found to be ≤10% when obtained from line width measurements and ≤20% for IT and SST measurements. Errors in k for total line shape analysis were determined by the upper and lower bounds of the rate constants that lead to ascertainable disagreements with the experimental spectra and were less than ±30%.[27] For a single coalescence measurement an uncertainty of ±3 degrees in the value of T_c corresponds to nearly ±50% in k and to ca. ±0.3 kcal/mol in $\Delta G^{\ddagger}$, although values obtained from Figure 1 are probably closer to ±40% and ±0.2 kcal/mol in k and $\Delta G_{r.i.}^{\ddagger}$, respectively.

Computational Methods. Ab initio molecular orbital calculations and geometry optimizations were performed with the GAUSSIAN 92 series of programs[13] at the Hartree−Fock (HF) level of theory with the 3-21G$^{(*)}$[12] basis set. Fully optimized geometries of the ground states and ring inversion transition states were shown to have zero and one imaginary frequency, respectively, by analytical frequency analysis.

Acknowledgment. We thank the National Science Foundation, the Carnegie Mellon SURG program, and the Swedish Natural Science Research Foundation for partial support of this research.

Supporting Information Available: Tables of rate constants obtained at various temperatures (5 pages, print/PDF). See any current masthead page for ordering information and Web access instructions.

JA980931Z

(26) Freeman, R.; Kempsell, S. P.; Levitt, M. H. *J. Magn. Reson.* **1980**, *38*, 453.

(27) Binsch, G.; Kessler, H. *Angew. Chem., Int. Ed. Engl.* **1980**, *19*, 411.

(28) Hu, N.; Gong, L.; Jin, Z.; Chen, W. *J. Organomet. Chem.* **1998**, *352*, 61.